

## Immunohistochemical and Immunocytochemical Localization of Amylase in Rat Parotid Glands and von Ebner's Glands by Ion Etching-Immunoscanning Electron Microscopy

Junko Yahiro<sup>1</sup>, Tetsuichiro Inai<sup>1</sup>, Akihito Tsutsui<sup>2</sup>, Atsuko Sato<sup>1</sup>, Toshikazu Nagato<sup>1</sup>, Kunihiisa Taniguchi<sup>1</sup>, Eichi Tsuruga<sup>1</sup> and Yoshihiko Sawa<sup>1</sup>

<sup>1</sup>Department of Morphological Biology, Fukuoka Dental College and <sup>2</sup>Department of Preventive and Public Health Dentistry, Fukuoka Dental College, 2-15-1 Tamura, Sawara-ku, Fukuoka 814-0193, Japan

Received December 1, 2010; accepted June 23, 2011; published online August 10, 2011

The distribution of amylase in rat parotid glands and von Ebner's glands was examined using ion etching-immunoscanning electron microscopy, which enables both light and electron microscopic observations of identical semi-thin resin sections immunolabeled with anti- $\alpha$ -amylase and immunogold in association with silver enhancement. At the light microscopic level, most acinar secretory granules (SG) and striated duct secretions of parotid glands were strongly stained dark brown. In von Ebner's glands, acinar SG and duct secretions were weakly to strongly stained light to dark brown. At the electron microscopic level, labeling was observed as bright gold-silver particles. The labeling intensity of acinar SG of parotid glands was higher than that of von Ebner's glands. In parotid glands, weak labeling of SG in transitional cells between acini and intercalated ducts, very weak labeling of SG in intercalated ducts, and strong labeling of striated duct secretions were observed. In von Ebner's glands, the secretions and some SG of interlobular ducts were strongly labeled compared to those of intralobular ducts and SG of acini. Less amylase was synthesized in von Ebner's acini compared to parotid acini, whereas von Ebner's ducts may secrete significantly more amylase to modify saliva than parotid ducts.

**Key words:** amylase, localization, parotid gland, von Ebner's gland, scanning electron microscopy

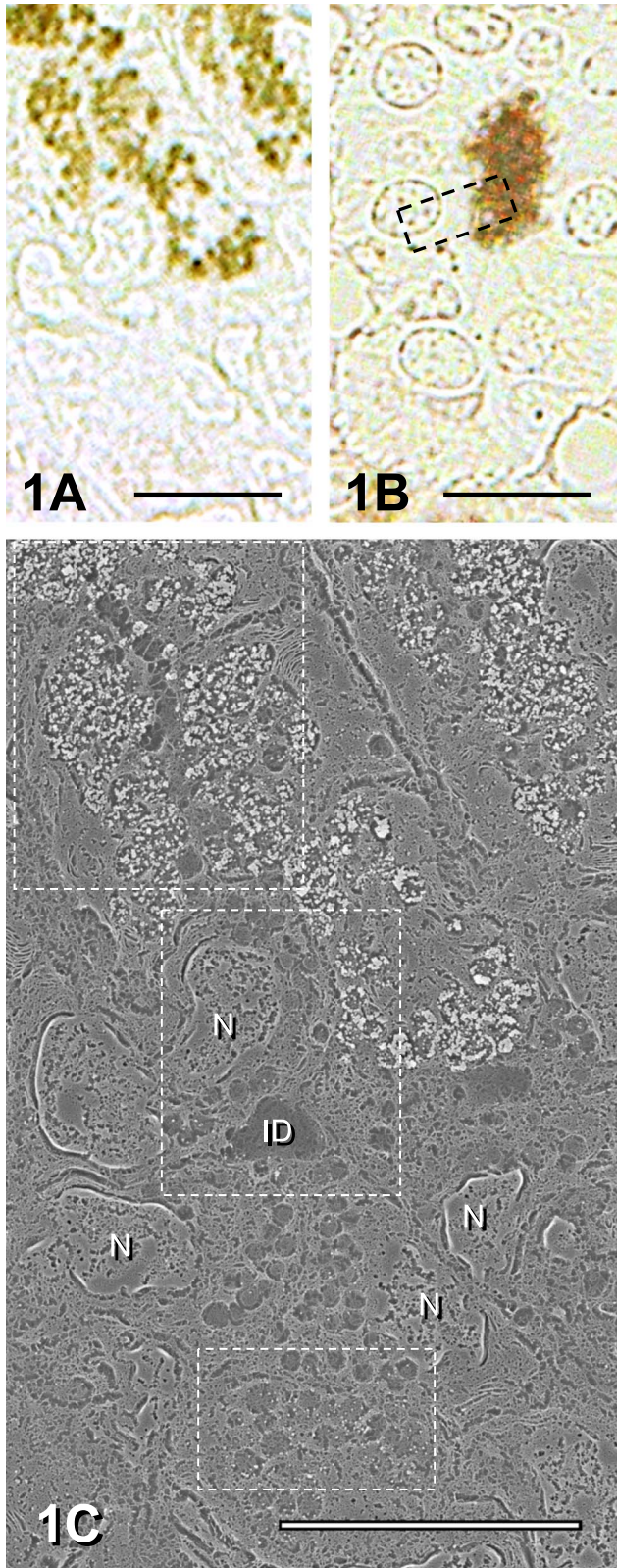
### I. Introduction

Major and minor salivary glands play a special role in the oral cavity, depending on their secretory materials and their location. The activity of amylase, a well-known enzyme, has been detected in major salivary glands of several mammals [14]. Genes encoding amylase and von Ebner's gland proteins have shown significantly higher expression in rat parotid gland than in other rat major salivary glands [22]. Immunocytochemical labeling has revealed the presence of amylase in the secretory granules (SG) of serous acinar cells in the parotid glands of such species as human [29, 32, 33] and rodent, including rat [4, 7, 8, 16, 17, 31,

35, 36, 41, 42]. However, little is known about the mechanisms of amylase secretion and the localization of amylase in ducts. Localization of amylase was found not in the submandibular glands and sublingual glands of other major salivary glands of rat and in the lingual mucous glands (Weber's glands) of minor salivary glands of rat [46]. Amylase, however, has been purified from the lingual serous glands (von Ebner's glands) of rat minor salivary glands [4]. Amylase secretion from rat von Ebner's glands is regulated by the parasympathetic nerve [3], while that from rat parotid glands is regulated by the sympathetic nerve [41]. Therefore, it is suspected that von Ebner's glands differ from parotid glands in terms of the mechanism and role of amylase secretion. One immunohistochemical study involving an enzymatic method has been reported [24]. However, as far as we know, there is no report of the immunocytochemical localization of amylase in von Ebner's glands.

Correspondence to: Tetsuichiro Inai, Department of Morphological Biology, Fukuoka Dental College, 2-15-1 Tamura, Sawara-ku, Fukuoka 814-0193, Japan. E-mail: tinaitj@fdcn.ac.jp

Recently, ion etching-immunoscanning electron microscopy (IE-immunoSEM) has been developed [45]. In the IE-immunoSEM protocol, resin is physically removed from the surface of semi-thin sections immunolabeled with



protein gold and subjected to silver enhancement, exposing the tissue surface for SEM observation. IE-immunoSEM enables both light and electron microscopic observations of identical semi-thin resin sections at low to high magnification (30,000 $\times$ ) [45]. Other immunoSEM techniques, such as SEM secondary and backscattered electron imaging, enable observation at  $\sim$ 3,000 $\times$  by means of osmium staining [21] or sodium hydroxide maceration [29] for chemical treatment, as well as observation at high magnification by means of EDTA decalcified fracture without silver enhancement [12].

IE-immunoSEM was conducted to investigate the immunocytochemical localization of amylase in the acini and ducts of rat von Ebner's glands in comparison with that of rat parotid glands. This is an optimal technique for detecting distributions over a wide area and localization in inner cellular organelles. The structures of interesting organelles, such as SG, are readily detected by light microscopy (LM) at low magnification and examined in detail at high magnification by SEM using the same section [5].

## II. Materials and Methods

### *Tissue preparation*

Five adult male Sprague-Dawley rats (six month after birth: Jackson laboratory, Japan) were anesthetized with sodium pentobarbital (25 mg/kg) and then perfused via the left ventricle with fixative containing 2.5% formaldehyde and 1% glutaraldehyde in 0.1 M phosphate buffer (pH 7.3). Parotid glands and von Ebner's glands were removed, cut into small pieces, continuously fixed for a total of 3 hr at 4 $^{\circ}$ C, and then rinsed with buffer. The experiment was conducted with the approval of our institutional animal ethics committee. After dehydration in ethanol (up to 80%), the specimens were embedded at 50 $^{\circ}$ C in LR White resin (hard: London Resin, England). Semi-thin sections (1.5  $\mu$ m thickness) were cut with a diamond knife and mounted on glass slides (aminosilane-coated: Matsunami Glass Industries Ltd., Osaka, Japan) for immunohistochemical processing [2, 9].

### *Immunostaining*

The semi-thin sections were hydrated with phosphate-buffered saline (PBS) for 30 min, covered with blocking

**Fig. 1.** (A & B) Immunolight micrographs of rat parotid gland. Secretory granules in acinar cells in Figure 1A and secretory materials in striated duct cavity in Figure 1B are strongly stained dark brown for amylase by protein gold labeling with the silver enhancement method; 2,000 $\times$ . (C) Immunoscanning electron micrograph of rat parotid gland. Ion etching was performed on the immunostained section. Same area as Figure 1A. Acinar SG are labeled with bright gold-silver particles for amylase. Unstained portion of Figure 1A is recognizable as intercalated duct (ID) that has dark small SG in apical cytoplasm. N: Nucleus; 4,000 $\times$ . Bars=10  $\mu$ m.

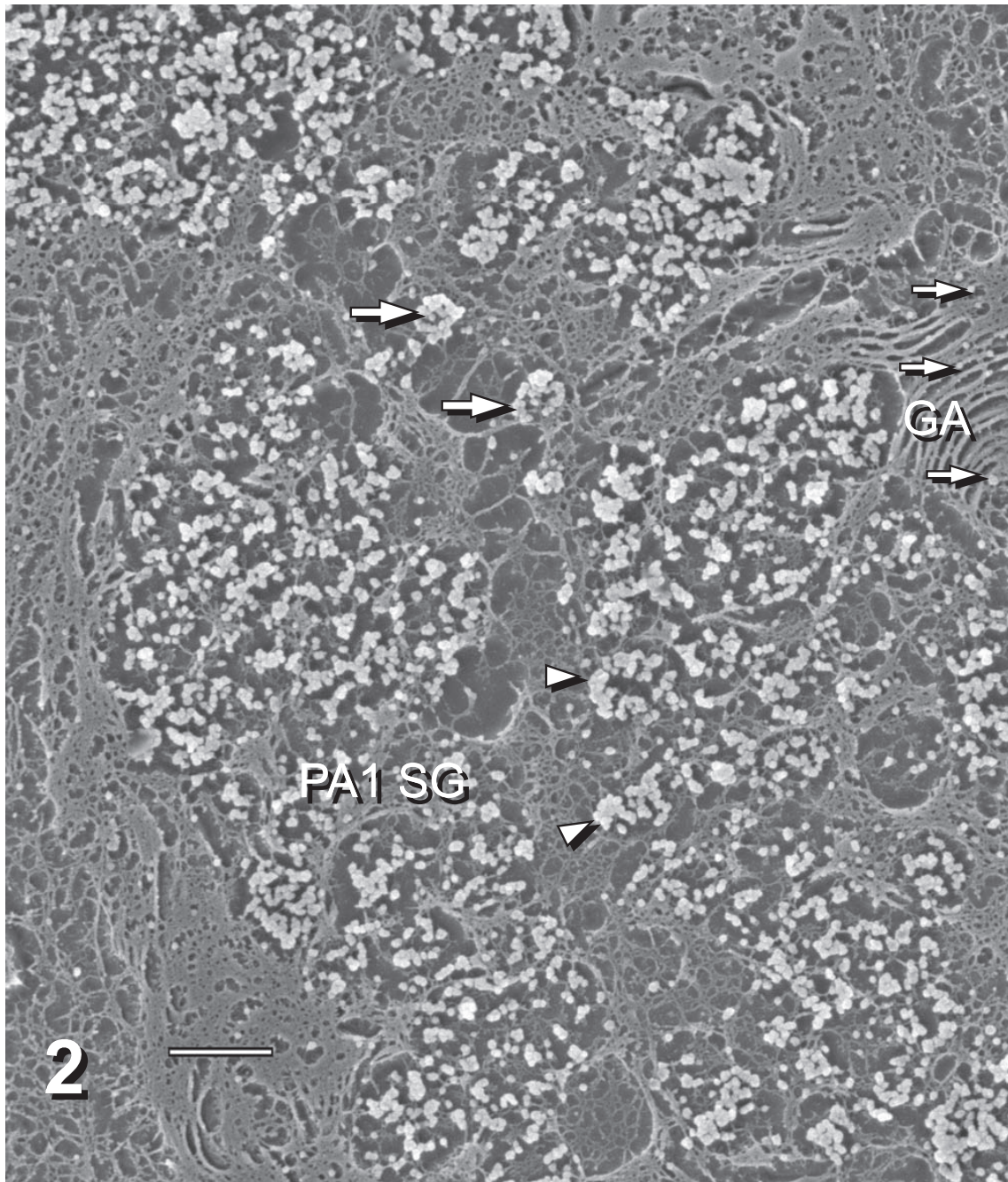


**Fig. 2.** IE-immunoSEM of rat parotid gland. High magnification of the top boxed region in Figure 1C. Parotid acinar typical SG (PA1 SG: 0.5–1  $\mu\text{m}$  in diameter) are strongly labeled with many electron-reflective gold-silver particles (100 nm in diameter). Dispersion of labeled contents is seen at lumen (arrowheads). Labeled spherules are discharged at the apical membrane of the cell (arrows). Labeling particles over Golgi apparatus (GA) are few; 15,000 $\times$ . Bar= 1  $\mu\text{m}$ .

solution consisting of 1% bovine serum albumin (BSA) in PBS for 30 min, and incubated overnight at 4°C with rabbit anti-human  $\alpha$ -amylase (Sigma, St. Louis, MO, USA) diluted 1:20 with 1% BSA in Tris buffered saline (TBS). The sections were rinsed for 20 min three times with buffer (0.05 M TBS+0.3 M NaCl+0.1% Tween 20: TBST), incubated for 90 min at room temperature with protein A/G gold conjugate 5 nm LM (British Biocell International: BBI,

Cardiff, UK, 1:150 dilution with 1% BSA-TBS), rinsed with TBST for 15 min twice and then with PBS for 15 min twice, washed for 2 min with distilled water jet, enhanced for 10 min (silver enhancer, BBI, Cardiff, UK: equal amount of initiator and enhancer mixture), washed for 2 min with distilled water jet, and dried. As immunostaining controls, normal rabbit serum (Dako Corp., Carpinteria, CA, USA) and antiserum pre-absorbed with human  $\alpha$ -amylase (Sigma,

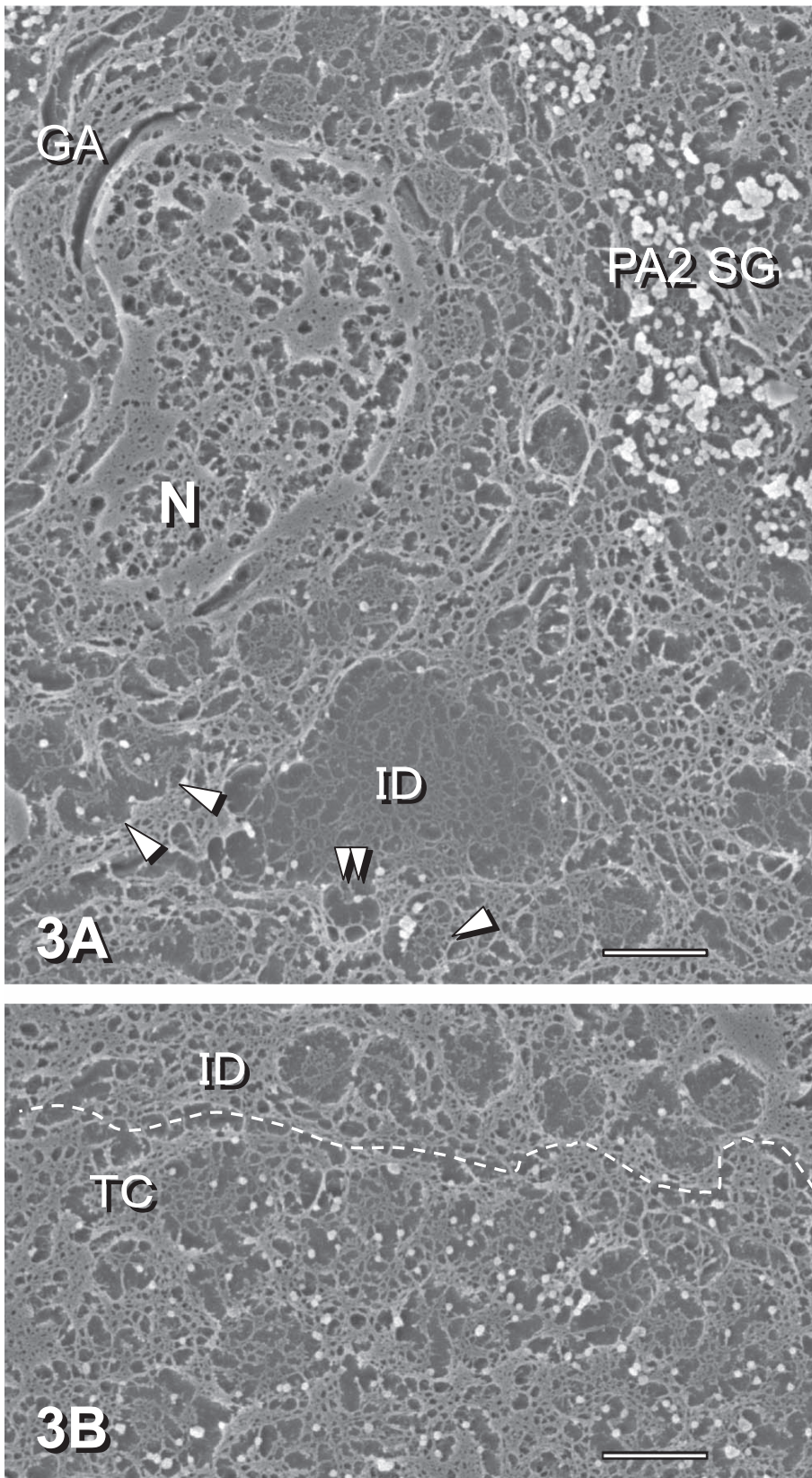


**Fig. 3.** IE-immunoSEM of rat parotid gland. High magnification of the (A) middle and (B) bottom boxed regions in Figure 1C; 15,000 $\times$ . (A) Strong labeling of peripheral zone with somewhat central zone in parotid acinar occasional SG (PA2 SG) is observed. A few particles over some small SG (arrowheads) are observed in the apical cytoplasm of intercalated duct (ID). At the luminal membrane, some labeled SG are exocytosed by merocrine secretion (double arrowheads). GA: Golgi apparatus, N: Nucleus. (B) Weak labeling of SG of a transitional cell (TC) adjacent to the ID cell. The SG in TC are larger and more electron-reflective than the SG in the ID cell. Bars=1  $\mu$ m.

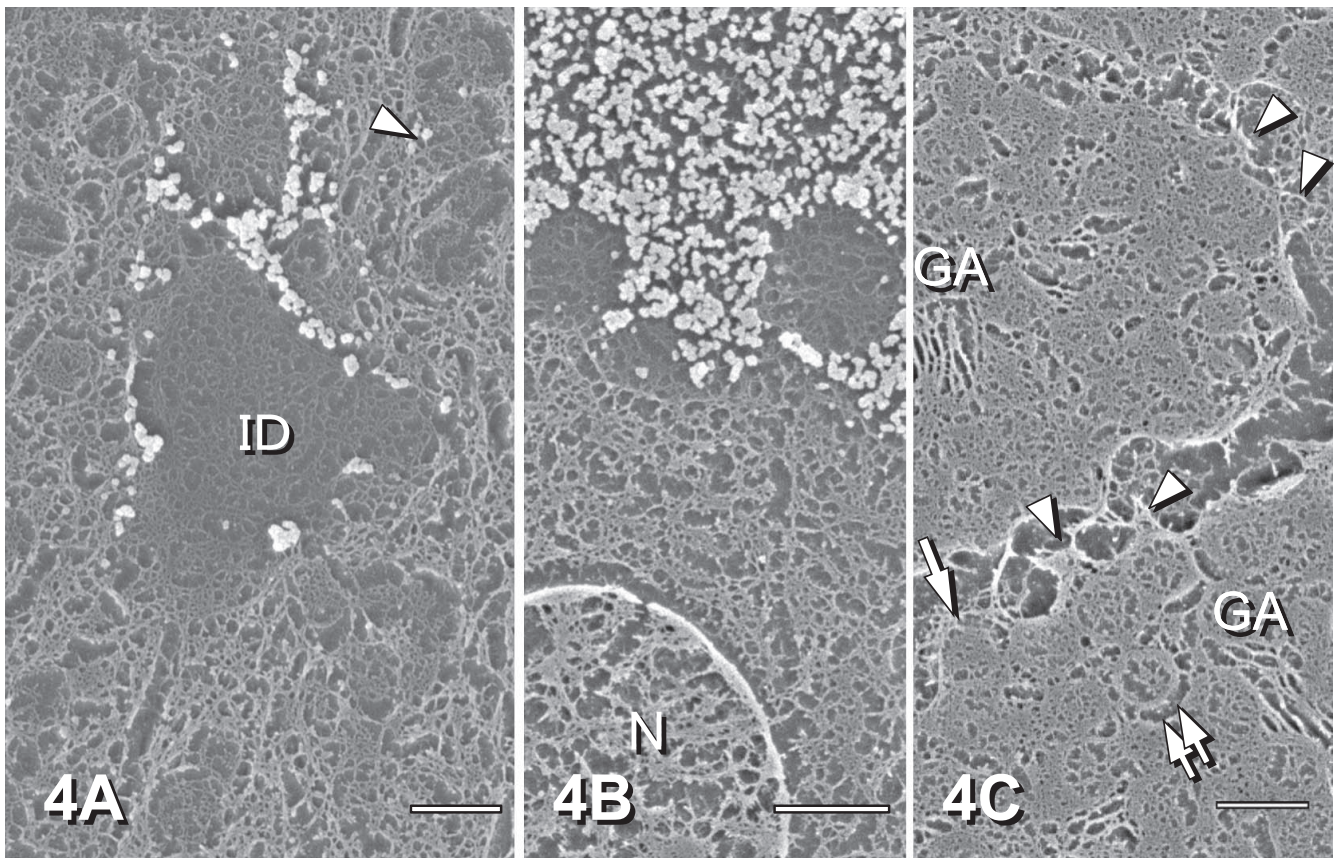


**Fig. 4.** IE-immunoSEM of rat parotid glands. (A) Intercalated duct (ID). Secretory material on apical membranes is labeled sporadically. Arrowhead indicates a few labeling particles on apical small SG; 12,000 $\times$ . (B) Striated duct cavity. Same as the boxed region in Figure 1B. Secretory material in luminal cavity is labeled strongly, but spherules on luminal membrane are unlabeled. N: Nucleus; 15,000 $\times$ . (C) Control involving anti-amylase absorbed to amylase displays few labeling. In usual acinar cells, SG are filled with amorphous structures and the contents are dispersed into the luminal cavity (arrowheads). In occasional acinar cells, some SG contain peripheral ring structures (double arrows). Spherical material is excreted (arrow). GA: Golgi apparatus; 12,000 $\times$ . Bars=1  $\mu$ m.

St. Louis, MO, USA) were used, instead of anti-amylase.

Immunostained sections were photographed with an Olympus BX51 microscope equipped with an Olympus DP12 digital camera.

#### *Ion etching for SEM*

Immunostained sections on glass slides were trimmed (5 mm<sup>2</sup>), attached with carbon seal to aluminum blocks, and subjected to mild IE (etching time 30 min, ionization voltage 350 V DC, operating vacuum 38 Pa, electrode clearance 8 cm: Ion coater IB-5, Eiko Japan), as described previously [45]. After coating with platinum (ion coater IB-5, Eiko Japan), secondary electron imaging of specimens was conducted on a field emission scanning electron microscope (JEOL JSM-6330F SEM, parameters were as follows: accelerating voltage, 5.0 kV; probe current,  $1.5 \times 10^{-10}$ – $3.2 \times 10^{-11}$  amps (emission current, 12.0  $\mu$ A); working distance, 15 mm; objective aperture, 50–70  $\mu$ m). Micrographs were obtained at an initial magnification of 2,000–10,000; subsequently, the micrographs were photographically enlarged to a magnification of 4,000 $\times$  to 15,000 $\times$ .

#### *Statistical analysis*

Labeling density was determined by counting gold-silver particles/ $\mu$ m<sup>2</sup> on electron micrographs printed at a final magnification of 15,000 $\times$ . In parts where two or more particles accumulated, the particle having a diameter of 100 nm was counted as one particle.

The cellular compartments of parotid and von Ebner's glands, for which labeling was estimated (values in parentheses are the number of each cellular compartment examined), were as follows: in the case of parotid glands, typical (30) and occasional (20) SG and Golgi apparatus (17) in acinar cells, SG in transitional cells (10), SG (31) and secretory material (11) in intercalated ducts, and secretory material in striated duct luminal cavities (33); in the case of von Ebner's glands, typical (25) and occasional (15) SG and Golgi apparatus (10) in acinar cells, SG (9) and secretory material (15) in intralobular ducts, and SG (20) and secretory material (10) in interlobular ducts. Data were analyzed with one-way ANOVA followed by DONNET. Labeling density in each of the parotid and Ebner's typical acinar SG that were usually found was considered as control.

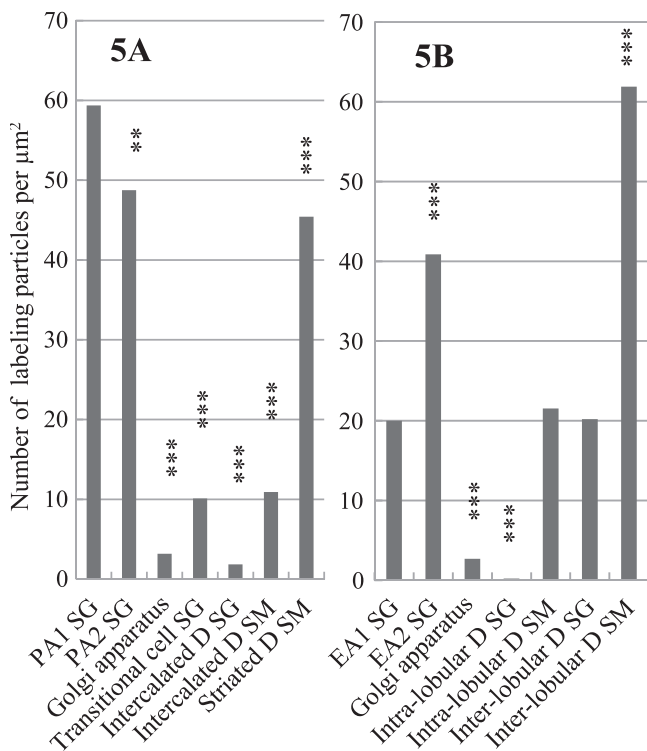


**Fig. 5.** Labeling density of amylase in the cellular compartments of (A) parotid glands and (B) von Ebner's glands. Each of typical acinar SG was considered as control and compared to other cellular compartments. (\*\* $P < 0.01$ , \*\*\* $P < 0.001$ ). D SG: duct secretory granules, D SM: duct secretory material, EA1: von Ebner's acinar typical, EA2: von Ebner's acinar occasional, PA1: parotid acinar typical, PA2: parotid acinar occasional.

### III. Results

#### Localization of amylase in parotid glands

LM (Fig. 1): On semi-thin sections immunostained for amylase by the 5 nm protein gold method followed by silver enhancement, most acinar SG were strongly stained

dark brown. Intercalated ducts were unstained and obscure (Fig. 1A). Striated duct secretions were stained dark brown (Fig. 1B).

IE-immunoSEM (Figs. 2–4): SEM secondary electron imaging observation of the same area in the same sections immunostained at LM level followed by IE revealed that acinar SG were labeled with many bright gold-silver particles. The gold-silver particles appeared black and electron-dense by TEM and brightly electron-reflective and white by SEM. Intercalated ducts were observable even at low magnification because contrast was produced by IE (Fig. 1C).

In intermediate to high-magnification SEM, many gold-silver labeling particles (100 nm in diameter) were observed within the acinar SG (Fig. 2). In parotid acinar typical SG (PA1 SG: 0.5–1  $\mu\text{m}$  in diameter), labeling particles were present over inner whole. In parotid acinar occasional SG (PA2 SG), the peripheral zone and the somewhat central zone were selectively labeled (Fig. 3A). At apical surfaces, the dispersion of labeled contents of SG usually occurred and the excretion of labeled spherules occasionally occurred (Fig. 2). Golgi apparatus was very weakly labeled. Nuclei were hardly labeled.

Intercalated duct cells had apical small and dark SG (0.5–0.7  $\mu\text{m}$  in diameter) and Golgi apparatus (Figs. 3A, 3B and 4A). Some intercalated duct SG were labeled with a few particles (Figs. 3A and 4A). At the luminal membrane, occasional SG with a few labeling particles were exocytosed by merocrine secretion (Fig. 3A). Sporadic labeling was observed on the luminal membrane of some intercalated ducts (Fig. 4A). There were few labeling particles on Golgi apparatus (Fig. 3A).

SG in transitional cells that were located adjacent to intercalated duct cells were larger, more electron-reflective, and more densely labeled than SG in intercalated duct cells (Figs. 1C and 3B).

In striated duct luminal cavities, labeling of secretory material was strong (Fig. 4B). Unlabeled spherules protruded into the cavities.

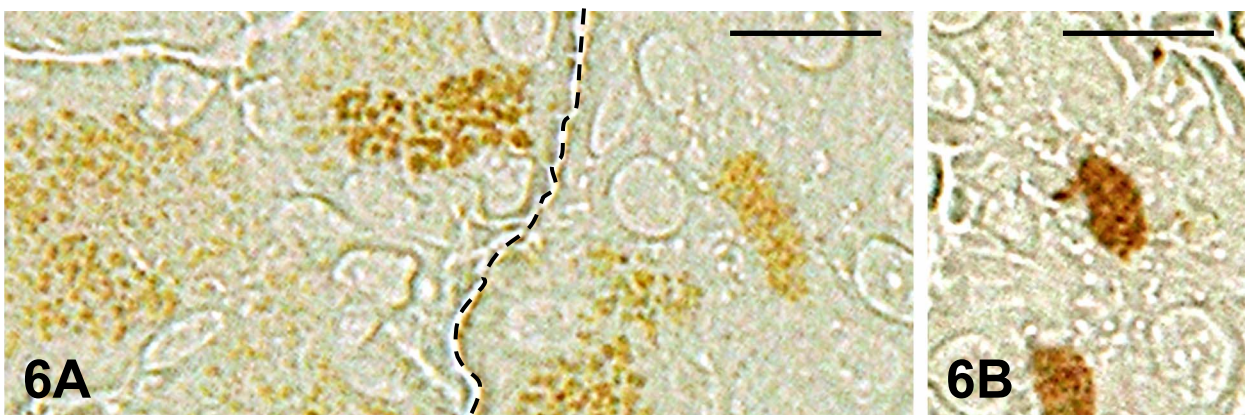


**Fig. 6.** Immunohistochemical (LM) of rat von Ebner's glands; 2,000 $\times$ . (A) SG in most acinar cells shown on the left and secretory material in intralobular duct cavity shown on the right side of the broken line are weakly stained light brown. SG in some acinar cells are moderately stained brown. (B) The contents of the interlobular duct cavity are strongly stained dark brown. Bars=10  $\mu\text{m}$ .

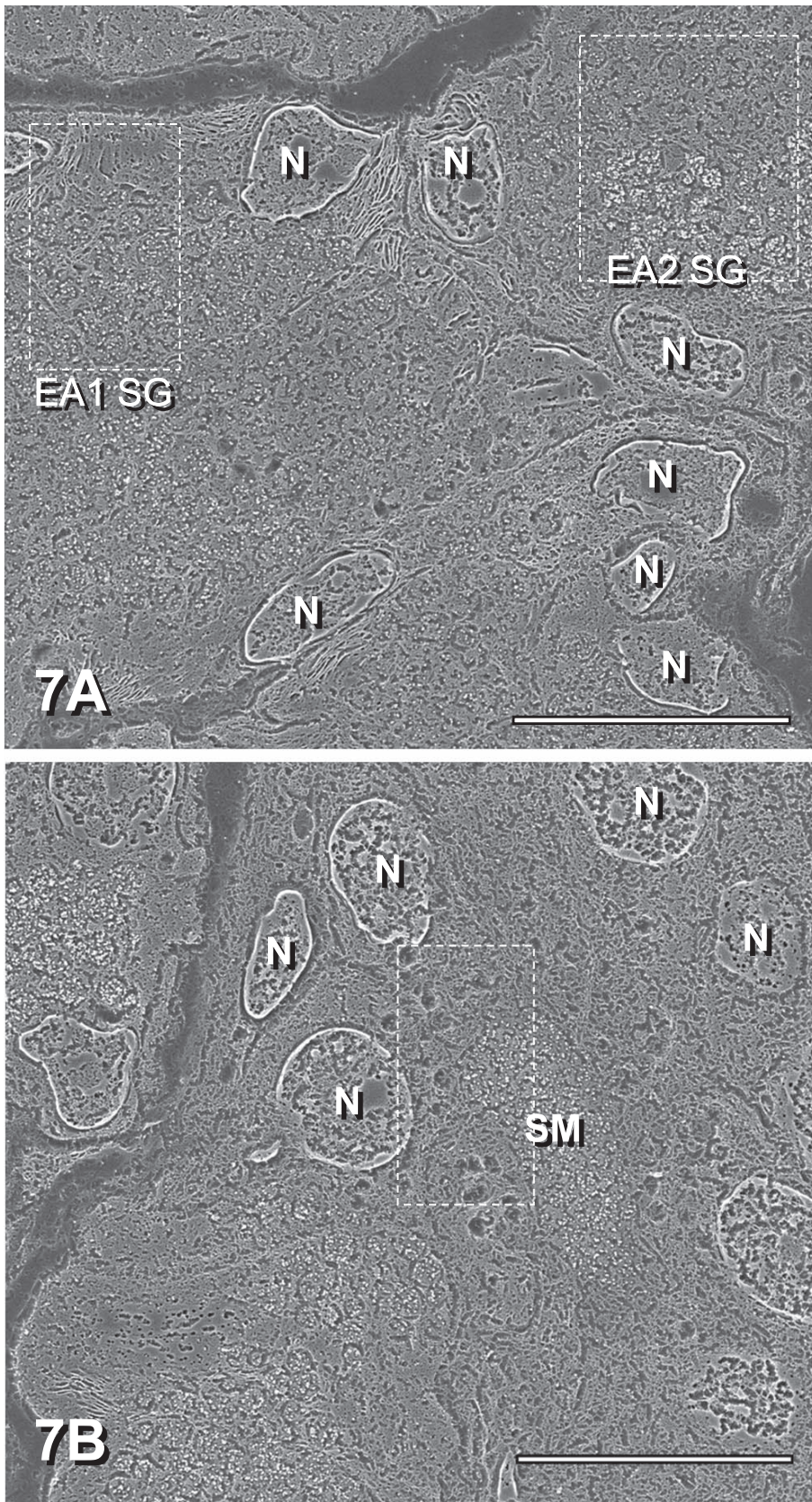


**Fig. 7.** IE-immunoSEM. Identical areas with the (A) left and (B) right half sides in Figure 6A. N: Nucleus; 4,000 $\times$ . (A) Acini. Moderate labeling of von Ebner's acinar occasional SG (EA2 SG) in the boxed region on the right side. Weak labeling of other von Ebner's acinar typical SG (EA1 SG). (B) Intralobular duct. Apical dark vesicles and weakly labeled SM are observed. Bars=10  $\mu$ m.

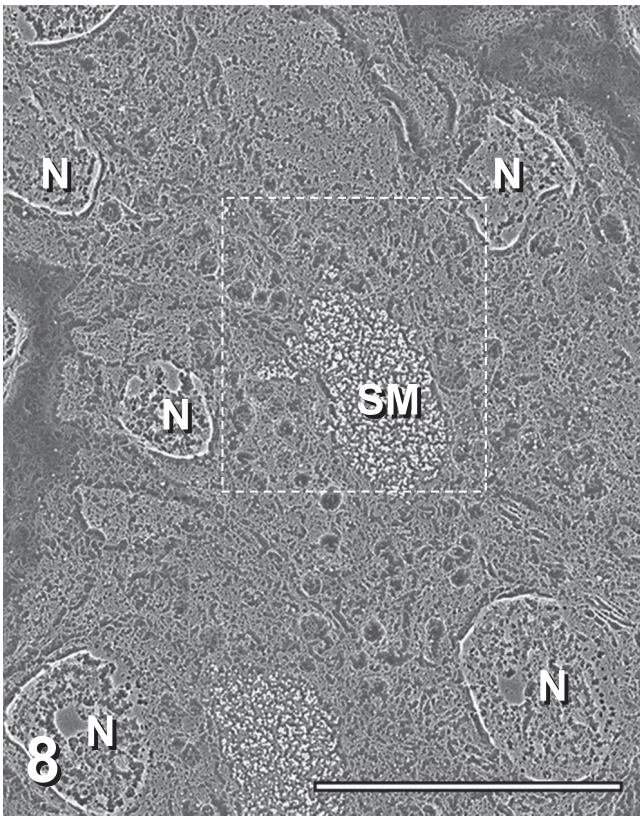


**Fig. 8.** IE-immunoSEM. Identical area with Figure 6B. Interlobular duct. Apical dark vesicles and strongly labeled SM are observed. N: Nucleus; 4,000 $\times$ . Bar=10  $\mu$ m.

Immunolabeling controls, including the pre-absorption test in which anti-amylase pre-absorbed with amylase was used instead of anti-amylase, showed no specific reaction (Fig. 4C). Most acinar SG were homogeneous, occupied comparatively low electron-dense and amorphous structures, and corresponded to PA1 SG. Some acinar SG were heterogeneous, had peripheral halos, and corresponded to PA2 SG. The contents of unlabeled acinar SG were more electron-reflective (Fig. 4C) than those of transitional cell SG and intercalated duct SG (Figs. 3B and 4A).

According to statistical analysis (Fig. 5A) in which PA1 SG served as the control, amylase labeling density in PA1 SG was the highest, and this was followed by that in PA2 SG, that in striated duct secretory material, and either that in intercalated duct secretory material or that in transitional cell SG. It was revealed that amylase in parotid glands is synthesized mainly in the acini, accumulates minimally in the intercalated ducts, and passes through the striated duct cavities.

#### *Localization of amylase in von Ebner's glands*

LM (Fig. 6): Acinar SG in von Ebner's glands were weakly stained light brown to brown compared with those in parotid glands. Secretions in intralobular duct cavities were weakly stained light brown, while those in interlobular

duct cavities were strongly stained dark brown.

IE-ImmunoSEM (Figs. 7–9): In intermediate to high-magnification SEM, intralobular ducts were clearly distinguished from acini. The labeling density on von Ebner's acinar typical SG (EA1 SG: 0.5–1  $\mu$ m in diameter) was lower than that on PA1 SG (Figs. 5, 7, and 9A). In some acini von Ebner's acinar occasional SG (EA2 SG) were labeled moderately (Figs. 7 and 9B). Golgi apparatus was labeled with a few particles (Fig. 9A).

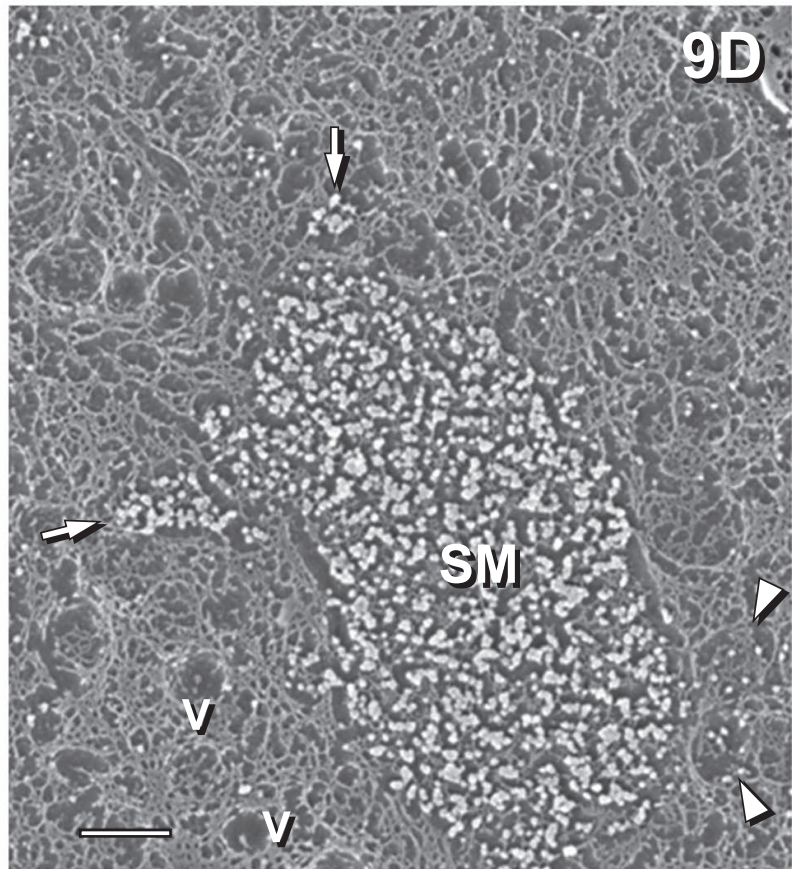
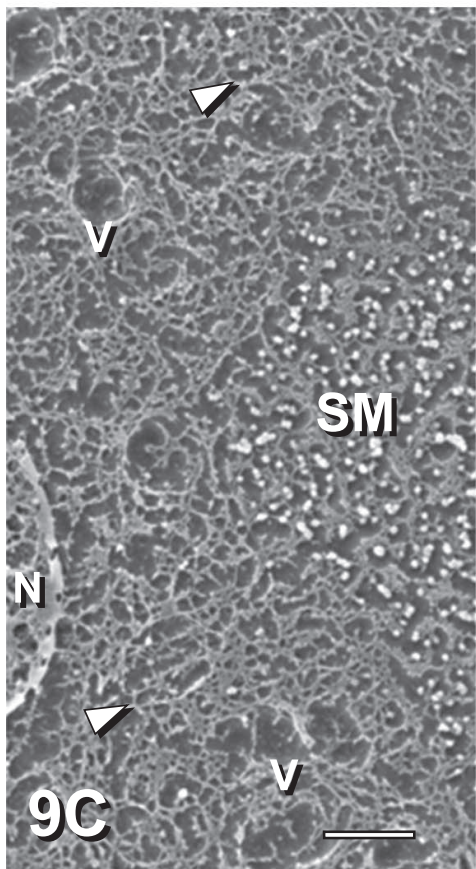
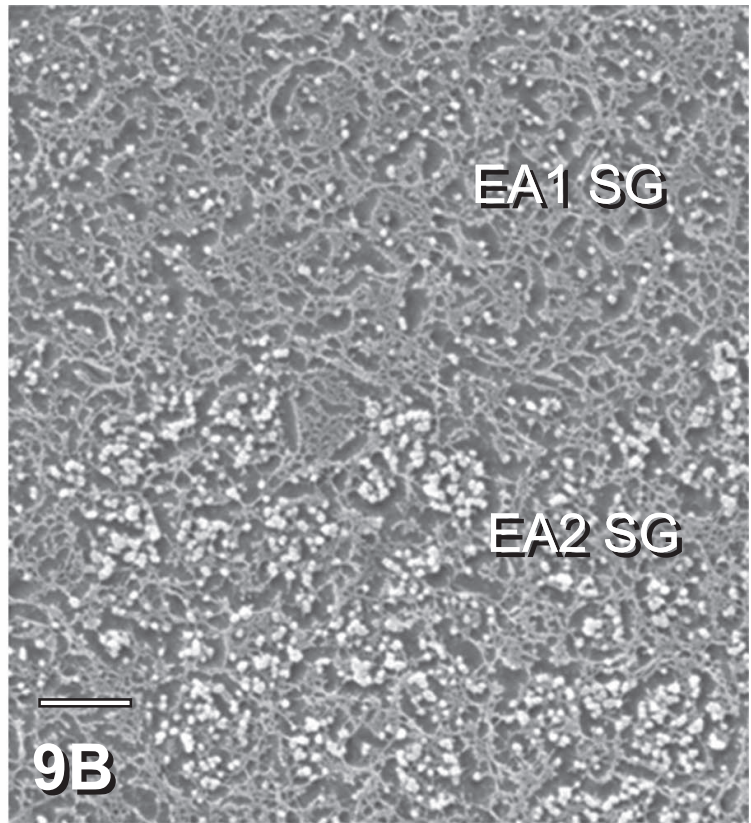
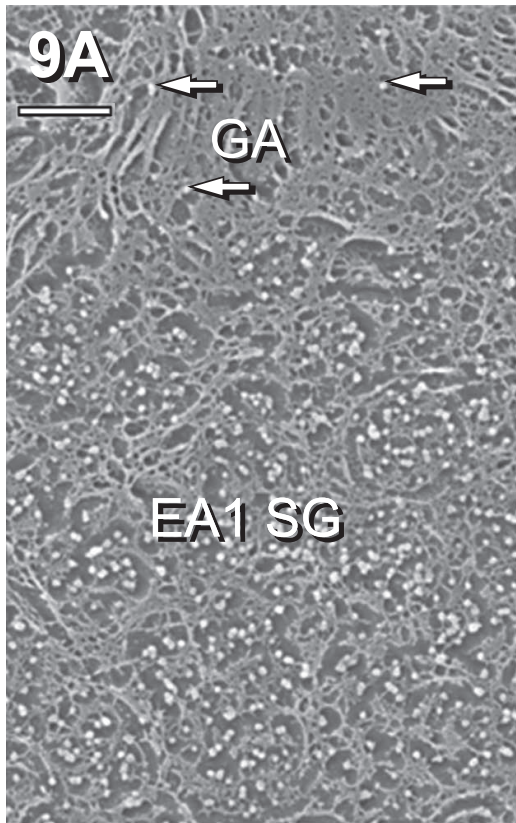
Intralobular duct cavities were relatively large and retained saliva (Figs. 7B and 9C). Both intralobular and interlobular duct cells had dark vesicles and small SG in the apical cytoplasm (Figs. 7B, 8, 9C and 9D). A few small SG of intralobular ducts were labeled weakly (Fig. 9C). The labeling density of secretory material in the intralobular duct cavities was similar to that of EA1 SG (Figs. 9A–9C). In interlobular ducts, some small SG were weakly to moderately labeled, while those occasionally fused to the lumen were strongly labeled (Fig. 9D). Secretory material in interlobular duct cavities were strongly labeled (Figs. 8 and 9D). Immunocytochemical control, in which normal serum was substituted for the primary antibody, was essentially free of gold particles (data not shown).

According to statistical analysis, amylase labeling density in EA1 SG and EA2 SG was lower than that in PA1 SG and PA2 SG (Fig. 5). Compared with the amylase labeling density in EA1 SG, the density was higher in EA2 SG, the highest in interlobular duct secretory material, and not different in intralobular duct secretory material and interlobular duct SG (Fig. 5B). It was revealed that amylase labeling density in interlobular duct SG is similar to that in EA1 SG, and so the amount of amylase in interlobular duct secretory material is markedly increased (Fig. 5B).

## IV. Discussion

The IE process over semi-thin (LR white) resin sections can be visualized by SEM secondary electron imaging [5, 45]. Observation of an identical section at the LM level from low to intermediate or high magnification at the SEM level is possible. The localization of amylase in the acinar SG of parotid glands and von Ebner's glands was revealed, appearing as light to dark brown by light microscopy and

**Fig. 9.** IE-immunoSEM of rat von Ebner's glands; 12,000 $\times$ . Identical areas with (A) left and (B) right boxed regions in Figure 7A, (C) the boxed region in Figure 7B, and (D) the boxed region in Figure 8. (A) Typical acinar cell. Weak labeling within EA1 SG. Labeling particles over Golgi apparatus (GA) are few. (B) Typical acinar and occasional cells. In both cases of weak labeling on EA1 SG and moderate labeling on EA2 SG, particles are concentrated within each acinar SG. (C) Apical cytoplasm of an intralobular duct. Weak labeling on SM of duct cavity and very weak labeling on a small SG (arrow). (D) Apical cytoplasm of an interlobular duct cell. Strong labeling on SM and some small SG (arrows). Weak labeling on other small SG (arrowheads). No labeling on vesicles (v). Bars=1  $\mu$ m.



a few to many bright particles of gold-silver labeling by IE-immunoSEM. Those bright gold-silver labeling particles were reversely observed as electron-dense black particles by conventional TEM. Tissue preparations, such as the fixative, LR White resin embedding, protein gold labeling, and silver enhancement, and the IE process used in the present study of amylase in parotid glands and von Ebner's glands were the same as those in a previous study of insulin in pancreatic islets [45]. In the present case of salivary glands, IE prior to immunostaining was not performed so that the given contrast was weak. Nevertheless, no artifacts were observed because salivary glands are made of a single structure as an exocrine gland. In contrast, among the exocrine glands, the pancreas contained endocrine islets and therefore, artifacts are easily produced in the islets. In the case of the pancreas, IE prior to immunostaining is useful. However, in the case of the present salivary glands, this step is unnecessary. IE-immunoSEM produces images similar to TEM images, is a reliable and simple method, can use protein gold-silver stained semi-thin sections employed in LM, and does not require osmium, uranium, or lead.

In this study that focused on IE-immunoSEM of rat parotid acinar SG, amylase labeling was observed throughout the inside of PA1 SG and throughout the peripheral zone and the central zone of PA2 SG. Controls that exhibited no specific labeling revealed that the former SG contained weakly electron-reflective amorphous structures, and that the latter SG had peripheral halos. The contents of many SG and the peripheral zone within occasional SG were labeled. The above-mentioned amylase distribution in the two types of SG in rat parotid acinar cells has been described in an immunoTEM study [36]. The peripheral ring structure of heterogeneous SG has been reported in parotid acinar cells of not only rat [1] but also mouse [25], insectivorous yellow bat [38], and cat [18, 23]. Conventional TEM observation indicated that the structure of serous SG is species-dependent [38]. Meanwhile, high amylase activity was detected in the parotid glands of guinea pig, rat, human, mouse, gerbil, rabbit, and insectivorous bat [15]. It is common knowledge that amylase is localized in the dark part of a TEM image of the parotid acinar SG of rat [1, 16, 36], gerbil [13, 14], and human [33], and conversely in the reflective light part on a SEM secondary electron image similar to the present study of the rat.

In von Ebner's acinar cells subjected to IE-immunoSEM, the contents of SG were labeled, resembling the present case of SG in parotid acinar cells. However, the labeling intensity of the acinar SG in von Ebner's glands was lower than that in parotid glands.

There were two patterns of amylase excretion from the luminal surface of the present rat parotid acini: one involved the usual fusion with the lumen to disperse the contents of SG, and the other involved occasional discharge of spherical SG. Two patterns of initial salivary secretion in acini, namely, the dispersion of SG contents in rat von Ebner's glands [6] and rabbit parotid glands [23], and the discharge of protrusions in human parotid glands [26] and von Ebner's

glands [27] and cat parotid glands [23], have been reported. Okugawa and Fujii [23] reported that the discharged spherical SG were surrounded by a limiting membrane that was thought to disappear in time. As far as we know, the excretory forms of amylase have not been reported so far.

In the present study, SG in occasional cells that were adjacent to intercalated duct cells were weakly labeled. The size, density, and labeling intensity of occasional cell SG were intermediate between those of acinar SG and intercalated duct SG. Therefore, the occasional cells that were adjacent to the intercalated duct cells were considered to be transitional cells. Vugman and Hand [41] indicated that occasional intercalated duct cells located close to acini underwent differentiation into an acinus-like phenotype as a result of isoproterenol treatment, and that the SG of those cells were labeled with anti-amylase. Therefore, it is suggested that intercalated duct cells may differentiate into acinar cells also in normal physiological conditions.

The present intercalated duct cells contained SG, some of which were labeled with a few particles. SG were found in the intercalated duct cells of parotid glands of various mammals [37], such as rat [28, 37], rabbit [19, 23], cat [23], and human [37]. Beta-adrenergic isoproterenol induces amylase expression in intercalated duct cells [41]. However, our study is the first to report the labeling of intercalated duct SG in the non-stimulated ordinal case. This is because even a small amount of antigen was detectable by the 5 nm gold labeling followed by silver enhancement immunostaining technique used in this study. Little attention is given to intercalated duct cells as they have a nondescript appearance in conventional histological preparations, while large amounts of glycoconjugates and electrolytes are secreted in intercalated ducts [37]. Myoepithelial cells that regulate secretion flow were found not only around acini but also along the intercalated ducts of rat [20] and mouse [11] parotid glands. In contrast, the endocytosis of amylase by lysosomes and vesicles in pathological conditions [17], nerve stimulation [8], and liquid diet [7] has been reported. Through this study, we found that secretions on luminal membranes of the intercalated ducts were sometimes labeled. Therefore, it is suggested that even under normal physiological conditions, intercalated duct cells occasionally secrete a small amount of amylase.

In the luminal cavity of the present parotid striated ducts, labeling was concentrated in secretory material (saliva) derived from acini and not in spherules protruding from the lumen. The unlabeled spherical protrusions indicate that the striated duct cells excrete substances other than amylase, such as kallikrein, which is present in the striated duct cells [39] of many species, including rat [30] and monkey [43, 44].

Some SG were found in duct cells of von Ebner's glands of rat [6], rabbit [40], mouse, hamster, monkey [34], and human [10]. In this study, we observed that the von Ebner's duct cells contained small SG that were labeled with anti-amylase, similarly to parotid intercalated duct cells. This observation supports the idea that von Ebner's ducts

resemble parotid intercalated ducts [6]. Moreover, SG in von Ebner's distal duct (interlobular duct) were labeled more strongly than SG in parotid intercalated duct and similarly to typical SG in von Ebner's acini. Secretory material in von Ebner's interlobular duct cavities was more strongly labeled than secretory material in von Ebner's intralobular duct cavities.

It is concluded that rat von Ebner's interlobular duct cells play a more important role in producing amylase than rat parotid intercalated duct cells; that is, von Ebner's interlobular duct cells produce considerable amounts of amylase into von Ebner's initial saliva, which contains less amylase compared to parotid initial saliva. Therefore, it is supposed that parotid amylase plays a significant role in digesting starch to suppress adhesion to the vestibule surface and teeth. In contrast, von Ebner's amylase breaks down starch to promote the detection of sweet taste at the sulcus of lingual papilla in the oral cavity proper. Various studies are required in order to clarify these roles of amylase. The present IE-immunoSEM technique was optimal for analyzing labeling intensity. Further studies on gender differences in localization of amylase remain to be done.

## V. Acknowledgments

This work was supported by Grants-in-Aid for Scientific Research (13671930 and 16591852) from the Ministry of Education, Culture, Sports, Science and Technology of Japan, and by a Grant-in-Aid for Frontier Research from Fukuoka Dental College.

## VI. Conflict of Interest

All authors declare that there is no conflict of interest as regards the contents of this manuscript, including employment or personal financial interest.

## VII. References

- Amico, F. D., Skarmoutsou, E., Imbesi, R. M. and Sanfilippo, S. (2001) Early events of secretory granule formation in the rat parotid acinar cell under the influence of isoproterenol. An ultrastructural and lectin cytochemical study. *Eur. J. Histochem.* 45; 169–175.
- Bendayan, M. (1984) Protein A gold microscopic immunocytochemistry: methods, applications and limitations. *J. Electron Microsc. Tech.* 1; 243–270.
- Field, R. B. and Hand, A. R. (1987) Secretion of lingual lipase and amylase from rat lingual serous glands. *Am. J. Physiol.* 253; G217–225.
- Field, R. B., Spielman, A. I. and Hand, A. R. (1989) Purification of lingual amylase from serous glands of rat tongue and characterization of rat lingual amylase and lingual lipase. *J. Dent. Res.* 68; 139–145.
- Fujiwara, T., Shimizu, D., Kon, K., Isshiki, N., Tsunokuni, H. and Aoyagi, S. (2000) A new method for detecting and localizing cell markers endocytosed by fibroblasts in epoxy resin semi-thin sections using scanning electron microscopy combined with energy dispersive X-ray microanalysis after ion-etching. *J. Electron Microsc.* 49; 551–558.
- Hand, A. R. (1970) The fine structure of von Ebner's gland of the rat. *J. Cell Biol.* 44; 340–353.
- Hand, A. R. and Ho, B. (1981) Liquid-diet-induced alterations of rat parotid acinar cells studied by electron microscopy and enzyme cytochemistry. *Arch. Oral Biol.* 26; 369–380.
- Hand, A. R., Colman, M. R., Mazariegos, M. R., Lustmann, J. and Lotti, V. (1987) Endocytosis of proteins by salivary gland duct cells. *J. Dent. Res.* 66; 412–419.
- Hand, A. R. and Jungmann, R. A. (1989) Localization of cellular regulatory proteins using post embedding immunogold labeling. *Am. J. Anat.* 185; 183–196.
- Hand, A. R., Pathmanathan, D. and Field, R. B. (1999) Morphological features of the minor salivary glands. *Arch. Oral Biol.* 44; S3–S10.
- Hata, M., Amno, I., Tsuruga, E., Kojima, H. and Sawa, Y. (2010) Immunoelectron microscopic study of podoplanin localization in mouse salivary gland myoepithelium. *Acta Histochem. Cytochem.* 43; 77–82.
- Hincke, M. T., Ching, Y. C., Gerstenfeld, L. C. and McKee, M. D. (2008) Colloidal-gold immunocytochemical localization of osteopontin in avian eggshell gland and eggshell. *J. Histochem. Cytochem.* 56; 467–476.
- Ichikawa, M., Sasaki, K. and Ichikawa, A. (1977) Light and electron microscopic histochemistry of the serous secretory granules in the salivary glandular cells of the Mongolian gerbil (*Mongolian meridianus*) and rhesus monkey (*Macaca irus*). *Anat. Rec.* 189; 125–140.
- Ichikawa, M., Sasaki, K. and Ichikawa, A. (1989) Immunocytochemical localization of amylase in gerbil salivary gland acinar cells processed by rapid freezing and freeze-substitution fixation. *J. Histochem. Cytochem.* 37; 185–194.
- Junqueira, L. C., Toledo, A. M. and Doine, A. I. (1973) Digestive enzymes in the parotid and submandibular glands of mammals. *An. Acad. Bras. Cienc.* 45; 629–643.
- Login, G. R., Ku, T. and Dvorak, A. M. (1995) Rapid primary microwave-aldehyde and microwave-osmium fixation: improved detection of rat parotid acinar cells secretory granule  $\alpha$ -amylase using a post embedding immunogold ultrastructural morphometric analysis. *J. Histochem. Cytochem.* 43; 515–523.
- Lotti, L. and Hand, A. (1988) Endocytosis of parotid salivary proteins by striated duct cells in streptozotocin-diabetic rats. *Anat. Rec.* 221; 802–811.
- Menghi, G., Bondi, A. M., Accili, D. and Fumagalli, L. (1989) Ultrastructure and complex carbohydrate ultracytochemistry of the cat parotid gland. *Biol. Struct. Morphogen.* 2; 149–158.
- Menghi, G., Bondi, A. M., Marchetti, L. and Fumagalli, L. (1992) On the fine structure and complex carbohydrate cytochemistry of the rabbit parotid gland. *Biol. Struct. Morphogen.* 4; 1–10.
- Murakami, M., Nagato, T. and Tanioka, H. (1990) A scanning electron microscope study of myoepithelial cells in the intercalated ducts of rat parotid and exorbital lacrimal glands. *Okajimas Folia Anat. Jpn.* 67; 309–314.
- Nanci, A., Zaizai, S. and Smith, C. E. (1990) Routine use of backscattered electron imaging to visualize cytochemical and autoradiographic reactions in semi-thin plastic sections. *J. Histochem. Cytochem.* 38; 403–414.
- Nashida, T., Sato, R., Imai, A. and Shimomura, H. (2010) Gene expression profiles of the three major salivary glands in rats. *Biomedical Res.* 31; 387–399.
- Okugawa, J. and Fujii, H. (1990) Comparative anatomical study on the ductal systems of rabbit and cat parotid glands. *J. Meikai Univ. Sch. Dent.* 19; 21–42 (In Japanese with English abstract).
- Paliwai, A., Srikantan, S., Hand, A. R. and Redman, R. S. (2006) Histological and biochemical characterization of von Ebner's glands in the Syrian hamster; comparison with rat von Ebner's glands. *Biotech. Histochem.* 81; 139–149.
- Parks, H. F. (1961) On the fine structure of the parotid gland of

- mouse and rat. *Am. J. Anat.* 108; 309–329.
26. Riva, A., Valentino, L., Serenella, M., Lantini, S., Floris, A. and Riva, F. T. (1993) 3D structure of cells of human salivary glands as seen by SEM. *Microsc. Res. Tech.* 26; 5–20.
  27. Riva, A., Loffredo, F., Puxeddu, R. and Riva, F. T. (1999) A transmission electron microscope study of the human minor salivary glands. *Arch. Oral Biol.* 44; 527–531.
  28. Sato, A., Yahiro, J., Toh, H. and Miyoshi, S. (1983) Fine structure of the duct systems of the rat parotid gland. *J. Fukuoka D. C.* 10; 82–93 (In Japanese with English abstract).
  29. Shimoda, H., Kajiwara, T., Takahashi, Y. and Kato, S. (2002) Scanning electron microscopic observation of immunohistochemically specified stromal cells following the NaOH maceration method. *J. Electron Microsc.* 51; 137–139.
  30. Simson, J. A. and Chao, J. (1994) Subcellular distribution of tissue kallikrein and Na,K-ATPase  $\alpha$ -subunit in rat parotid duct cells. *Cell Tissue Res.* 275; 407–417.
  31. Sivakumar, S., Mirels, L., Miranda, A. J. and Hand, A. R. (1998) Secretory protein expression patterns during rat parotid gland development. *Anat. Rec.* 252; 485–497.
  32. Takano, K., Bogert, M., Maramud, D. and Lally, E. (1991) Differential distribution of salivary agglutinin and amylase in the Golgi apparatus and secretory granules of human salivary gland acinar cells. *Anat. Rec.* 230; 307–318.
  33. Takano, K., Maramud, D., Bennic, A., Oppenheim, F. and Hand, A. R. (1993) Localization of salivary proteins in granules of human parotid and submandibular acinar cells. *Critic. Rev. Oral Biol. Medic.* 230; 307–318.
  34. Takeda, S. (1976) The fine structure of von Ebner's gland in the rat, the mouse, the hamster, the monkey and the human fetus. *Jap. J. Oral Biol.* 18; 60–74 (In Japanese with English abstract).
  35. Tamaki, H. and Yamashina, S. (1994) Improved method for post-embedding cytochemistry using reduced osmium and LR White resin. *J. Histochem. Cytochem.* 42; 1285–1293.
  36. Tanaka, T., Gresik, E. W. and Barka, T. (1981) Immunocytochemical localization of amylase in the parotid gland of developing and adult rats. *J. Histochem. Cytochem.* 29; 1189–1195.
  37. Tandler, B. and Phillips, C. J. (1993) Structure of serous cells in salivary glands. *Microsc. Res. Tech.* 26; 32–48.
  38. Tandler, B., Nagato, T., Toyoshima, K. and Phillips, C. J. (1998) Comparative ultrastructure of intercalated ducts in major salivary glands: a review. *Anat. Rec.* 252; 64–91.
  39. Tandler, B., Gresik, E. W., Nagato, T., Toyoshima, K. and Phillips, C. J. (2001) Secretion by striated ducts of mammalian major salivary glands: review from an ultrastructural, functional, and evolutionary perspective. *Anat. Rec.* 264; 121–145.
  40. Toyoshima, K. and Tandler, B. (1986) Ultrastructure of von Ebner's salivary glands in the rabbit. *J. Submicrosc. Cytol.* 18; 509–517.
  41. Vugman, I. and Hand, A. R. (1995) Quantitative immunocytochemical study of secretory protein expression in parotid glands of rat chronically treated with isoproterenol. *Microsc. Res. Tech.* 31; 106–117.
  42. Whitson, S. W. and Hand, A. R. (1984) Isoproterenol-induced changes in glutathione metabolism in the rat parotid gland. *Arch. Oral Biol.* 29; 137–140.
  43. Yahiro, J. and Miyoshi, S. (1996) Immunohistochemical localization of kallikrein in salivary glands of the Japanese monkey, *Macaca fuscata*. *Arch. Oral Biol.* 41; 225–228.
  44. Yahiro, J. and Miyoshi, S. (2002) Distribution of kallikrein in striated duct cells monkey submandibular glands. *Arch. Oral Biol.* 47; 631–635.
  45. Yahiro, J. and Nagato, T. (2005) Application of ion etching to immunoscanning electron microscopy. *Microsc. Res. Tech.* 67; 240–247.
  46. Yahiro, J. and Nagato, T. (2006) Ion-etching immunoscanning electron microscopic observation of rat glands. *J. Dent. Res.* 85S; 87.

---

This is an open access article distributed under the Creative Commons Attribution License, which permits unrestricted use, distribution, and reproduction in any medium, provided the original work is properly cited.

---